RESEARCH ARTICLE

Synaptic connections of amacrine cells containing vesicular glutamate transporter 3 in baboon retinas

DAVID W. MARSHAK,[1,2] ALICE Z. CHUANG,[2] DREW M. DOLINO,[1,3] ROY A. JACOBY,[4]
WEILEY S. LIU,[1] YE LONG,[1] MICHAEL B. SHERMAN,[5] JAE M. SUH,[1] ALEJANDRO VILA,[2,3] AND
STEPHEN L. MILLS[2]

[1]Department of Neurobiology and Anatomy, University of Texas Medical School, Houston, Texas
[2]Department of Ophthalmology and Visual Science, University of Texas Medical School, Houston, Texas
[3]Graduate School of Biomedical Sciences, University of Texas Health Science Center at Houston, Houston, Texas
[4]Department of Ophthalmology, Baylor College of Medicine, Houston, Texas
[5]Department of Biochemistry & Molecular Biology, University of Texas Medical Branch, Galveston, Texas

Abstract

The goals of these experiments were to describe the morphology and synaptic connections of amacrine cells in the baboon retina that contain immunoreactive vesicular glutamate transporter 3 (vGluT3). These amacrine cells had the morphology characteristic of knotty bistratified type 1 cells, and their dendrites formed two plexuses on either side of the center of the inner plexiform layer. The primary dendrites received large synapses from amacrine cells, and the higher-order dendrites were both pre- and postsynaptic to other amacrine cells. Based on light microscopic immunolabeling results, these include AII cells and starburst cells, but not the polyaxonal amacrine cells tracer-coupled to ON parasol ganglion cells. The vGluT3 cells received input from ON bipolar cells at ribbon synapses and made synapses onto OFF bipolar cells, including the diffuse DB3a type. Many synapses from vGluT3 cells onto retinal ganglion cells were observed in both plexuses. At synapses where vGluT3 cells were presynaptic, two types of postsynaptic densities were observed; there were relatively thin ones characteristic of inhibitory synapses and relatively thick ones characteristic of excitatory synapses. In the light microscopic experiments with Neurobiotin-injected ganglion cells, vGluT3 cells made contacts with midget and parasol ganglion cells, including both ON and OFF types. Puncta containing immunoreactive gephyrin, an inhibitory synapse marker, were found at appositions between vGluT3 cells and each of the four types of labeled ganglion cells. The vGluT3 cells did not have detectable levels of immunoreactive γ-aminobutyric acid (GABA) or immunoreactive glycine transporter 1. Thus, the vGluT3 cells would be expected to have ON responses to light and make synapses onto neurons in both the ON and the OFF pathways. Taken with previous results, these findings suggest that vGluT3 cells release glycine at some of their output synapses and glutamate at others.

Keywords: Glycine, Gephyrin, Primate, Parasol, Midget

Introduction

Amacrine cells, inhibitory local circuit neurons of the inner retina, are clearly important for information processing in primate retina because their synapses are the most numerous in the inner plexiform layer (IPL) (Koontz & Hendrickson, 1987). Many distinct morphological types of amacrine cells have been described in primate retinas, but only a few have been described at the level of synapses between identified populations of neurons. Amacrine cells can be broadly divided into wide-field and narrow-field types. Narrow-field amacrine cells have relatively small dendritic fields and branch in two or more of the five strata that comprise the IPL. They typically use the neurotransmitter glycine and make inhibitory synapses onto bipolar cells, ganglion cells, and other amacrine cells. Several types of narrow-field amacrine cells have dendrites in both the inner strata of the IPL, where bipolar cells and ganglion cells that respond to increments in light intensity ramify, and in the outer strata of the IPL, where bipolar cells that respond to decrements in light intensity typically ramify (Wassle et al., 2009). The best-understood narrow-field amacrine cells in primates are AII cells, whose morphology and synaptic connections are very similar to those of other mammals (Wassle et al., 1995; Mills & Massey, 1999). A number of other types of narrow-field amacrine cells have been described morphologically in primates (Mariani, 1990; Kolb et al., 1992), but very little is known about their functions.

Address correspondence to: David W. Marshak, Department of Neurobiology and Anatomy, Medical School, University of Texas Health Science Center at Houston, PO Box 20708 Houston, TX 77225. E-mail: david.w.marshak@uth.tmc.edu

1

Here, we describe the synaptic connections of a type of narrow-field amacrine cell in baboon retina that contains immunoreactive vesicular glutamate transporter 3 (vGluT3) (Haverkamp & Wassle, 2004; Jusuf et al., 2005). Using light microscopic double and triple labeling, we showed that vGluT3 amacrine cells are not specialized to provide input to a particular type of retinal ganglion cell. Rather, they are presynaptic to both midget ganglion cells and parasol ganglion cells, including ON and OFF subtypes of each. The vGluT3 cells would also be expected to influence both the types of ganglion cells indirectly. The vGluT3 cells are presynaptic to axon terminals of DB3a bipolar cells, which are presynaptic to OFF parasol cells (Jacoby & Marshak, 2000; Puthussery et al., 2013). The vGluT3 cells interact with starburst amacrine cells that, in turn, provide input to ON parasol cells (Jacoby et al., 1996; Bordt et al., 2006). The vGluT3 cells also make contacts with AII amacrine cells, which are presynaptic to OFF midget ganglion cells (Grunert, 1997).

Materials and methods

Retinal ganglion cell injection with Neurobiotin

Baboon (*Papio anubis*) eyes were provided by the Southwest National Primate Research Center at the Texas Biomedical Research Institute (San Antonio, TX). Within 10 min of death, the animals were enucleated, the anterior half of the eye was cut away, and the vitreous humor was removed with fine forceps. The eyecups were stored in carboxygenated Ames medium (Sigma–Aldrich, St. Louis, MO) for approximately 4 h at 20°C. Under room light, the eyecups were cut into small pieces (5 mm × 5 mm) and the retina was isolated. It was placed on a black membrane filter paper, ganglion cell side up and superfused in carboxygenated Ames medium (Sigma–Aldrich) on an upright, fixed stage microscope, i.e., Olympus BX50WI or BX51WI microscope (Tokyo, Japan). Unused pieces were stored at room temperature in carboxygenated Ames medium and kept in the dark.

The pieces of retina were stained with a few drops of dilute acridine orange solution (Sigma–Aldrich). Glass microelectrodes were pulled with a Flaming-Brown horizontal micropipette puller (Sutter Instruments. Novato, CA), tip-filled with a mixture of 0.5% Lucifer Yellow-CH (L-453, Invitrogen, Carlsbad, CA) and 3.5% Neurobiotin (Vector Laboratories, Burlingame, CA) in 0.05 M PBS, and backfilled with 3 M LiCl. The electrode resistance was between 50 and 100 MΩ. Retinal ganglion cell somas were targeted based on their size and the intensity of acridine orange staining with a 40× water immersion objective. Several cells in each piece of retina were injected with Neurobiotin using 1 nA positive current at 2–3 Hz for 10–15 min using a Warner Instruments (Hamden, CT) 1 E-210 amplifier, and tracer was allowed to diffuse for 30 min at 35°C before fixation. Some ganglion cells were injected following the addition of 50 μM SCH23390 (Tocris Biosciences, Bristol, United Kingdom), an antagonist of the dopamine D1 receptor, to the superfusate to increase gap junctional coupling and label the tracer-coupled amacrine cells (Mills et al., 2007). After the last injection, retinal pieces were fixed in 4% paraformaldehyde in 0.1 M sodium phosphate buffer pH 7.4 for 30 min or else overnight and washed several times in PBS. Neurobiotin was visualized by incubating retinas with Alexa 488-conjugated or cyanine 3-conjugated streptavidin (Jackson Immunoresearch, West Grove, PA) 1:500 overnight using the same diluents as for the secondary antibodies (see below).

Immunolabeling with vGluT3 antibody

Baboon eyecups from the same source were immersion fixed in 0.1 M phosphate buffer (PB) pH 7.4 containing 4% paraformaldehyde (Sigma–Aldrich) for varying lengths of time. In some instances, 0.05–0.1% glutaraldehyde (EM grade, Ted Pella, Inc., Redding, CA) or 0.1% picric acid (Sigma–Aldrich) was included, and those retinas were pretreated with 1% sodium borohydride (Sigma–Aldrich) in PBS. The fixed retinas were isolated from the retinal pigment epithelium. To facilitate the penetration of the antibodies, the tissue fixed with glutaraldehyde or picric acid was treated with an ascending and descending series of graded ethanol solutions in PBS (10 min each 10, 25, 40, 25, and 10%). Most retinal pieces were embedded in 4.5% low-melting temperature agarose (Bio-Rad, Hercules, CA) in phosphate-buffered saline with 0.3% sodium azide (PBSa), and 40 or 50 μm vertical sections were cut using vibratome (Leica VT1000 S, Bannockburn, IL). Others were cryoprotected in 30% sucrose (Sigma Aldrich) in PBS and sectioned using a Microm HM505E cryostat (Thermo Fisher Scientific, Inc., Waltham, MA).

The tissue was rinsed three times in PBS after this and all other steps. It was pretreated with 5% Chemiblock (Millipore, Billerica, MA) and incubated in diluted primary antiserum or purified IgG at 4°C in PBSa with 0.3% triton X-100 (Sigma–Aldrich). Sections were incubated for a minimum of 7 days. In addition to rabbit antiserum against vGluT3 (donated by Prof. Reinhard Jahn, Max Planck Institute, Göttingen, Germany, 1:1000), the sections cut by vibratome were labeled using mouse monoclonal antibodies against parvalbumin (1:2,000, Swant, Bellinzona, Switzerland Catalog No. 235), calbindin (1:1000 Sigma–Aldrich Catalog No. C8666), gephyrin (1:1,000, Synaptic systems, Göttingen, Germany Catalog No. 147-011) or tyrosine hydroxylase (1:5,000, Sigma–Aldrich Catalog No. T2928); goat polyclonal antibodies against choline acetyltransferase (1:1000, Millipore Catalog No. AB144P), calretinin (1:1000, Millipore Catalog No. AB1550), or glycine transporter 1 (Biogenesis, Brentwood, NH Catalog No. 4710-8050) or else rat polyclonal antibody against γ-aminobutyric acid (GABA) (donated by Prof. David V. Pow, RMIT University, Melbourne, Australia, 1:1000).

Secondary antibodies were all raised in donkeys and affinity-purified. These include: anti-goat IgG conjugated to Cy3 (1:1000, Jackson Immunoresearch), anti-rabbit IgG conjugated to Alexa 488 (1:750; Molecular Probes, Eugene, OR) or biotin (1:00, Jackson Research Laboratories), and anti-mouse IgG conjugated to DyLight 649 (1:1000 Jackson Immunoresearch). Sections were incubated in secondary antibodies for 2 h at 20°C, and pieces of retina were left in secondary antibodies for 2 days at 4°C. Tissue was coverslipped in Vectashield mounting medium (Vector Laboratories, Burlingame, CA) with 4,6-diamino-2-phenylindole dihydrochloride (DAPI).

Confocal microscopy

The images were acquired using a Zeiss LSM 510 laser scanning confocal microscope (Carl Zeiss, Thornwood, NY). Fluorescent beads (TetraSpeck; Invitrogen, Carlsbad, CA) were used as reference standards to verify the colocalization of probes emitting different wavelengths of light in the same optical plane. All the sections were imaged with dye-appropriate filters. The images were acquired with 40× or 63× oil-immersion objectives as a series of optical sections 0.5–1.0 μm in step size. Each marker was assigned a pseudocolor, and the images were analyzed as single optical sections and as stacks of optical sections projected along the *y* or *z* axis. All the images were processed in Adobe Photoshop (Adobe Systems 9.0, San Jose, CA) to enhance brightness and contrast.

*Electron microscopic immunohistochemistry*

The eyecups from two baboons were fixed in 4% paraformaldehyde and 0.05% glutaraldehyde in 0.1 M PB for 60 min, and the retina was treated with sodium borohydride and ethanol. The 100-μm-thick sections cut by vibratome were prepared and labeled with anti-vGluT3 as described above except that an immunoperoxidase method was used (Gastinger et al., 2006). The tissue was treated with 1% osmium tetroxide (Electron Microscopy Sciences, Hatfield, PA) in PB for 60 min, dehydrated and embedded in Epon (Ted Pella, Inc., Redding, CA). Serial sections of 80–100 nm thickness were cut using a Reichert Ultracut E ultramicrotome (Leica Microsystems, Buffalo Grove, IL) collected on Formvar-coated, single-hole grids (Electron Microscopy Sciences), and stained with 1% aqueous uranyl acetate (Ted Pella, Inc.) for 20 min followed by 0.2% aqueous lead citrate (Reynolds, 1963) for 1–2 min. Labeled processes were photographed at 5000× using a JEOL 1400 electron microscope (JEOL USA, Peabody, MA). Statistical analyses were done using SAS (Cary, NC) software.

Results

Antibody to vGluT3 consistently labeled amacrine cell dendrites, as described previously (Haverkamp & Wassle, 2004; Jusuf et al., 2005). The dendrites had a generally vertical orientation, and they formed varicosities approximately 0.5 μm in diameter (Fig. 1A and 1B). The dendrites were organized into two broad plexuses whose depth in the IPL was specified as a percentage, with 0 being the inner nuclear layer and 100 being the ganglion cell layer. The plexus in the outer half of the IPL extended from approximately 20–40% of the IPL depth, and the plexus in the inner half extended from approximately 50–80% (Fig. 2). In some retinas, particularly when the retinas were fixed in 4% paraformaldehyde for only 30 min, labeled perikarya in the innermost row of the inner nuclear layer were also observed. There was also a relatively weak labeling of bipolar cell axon terminals under some conditions; these were clearly distinguishable from the labeled amacrine cell dendrites by their morphology. Based on previous work in human retinas, this may represent cross-reactivity with vGluT1 (Gong et al., 2006). These labeled bipolar cells were not studied further.

In the electron microscopic study, the amacrine cell dendrites containing immunoreactive vGluT3 were followed through a short series of sections, typically 8–10. At the sites of synapses, the membranes of both the pre- and the postsynaptic neurons were more electron-dense and more nearly parallel than nonsynaptic membranes, and there was electron-dense material in the space between them. In the figures, edges of the synaptic densities are indicated by black arrowheads in the unlabeled cells, whether they are pre- or postsynaptic. Synaptic ribbons are labeled with white arrowheads.

The neurons pre- and postsynaptic to the labeled amacrine cell dendrites were identified by their characteristic ultrastructure. Axon terminals of bipolar cells were identified by their abundant synaptic vesicles and their synaptic ribbons. Processes of amacrine cells contained fewer synaptic vesicles, and they were typically clustered at synapses. Ganglion cell dendrites were relatively electron-lucent and lacked presynaptic specializations (Dowling & Boycott, 1966). Bipolar cells were considered presynaptic to the labeled dendrites when a synaptic ribbon was present at the synapse; they were considered postsynaptic when there was no ribbon associated with the synapse. Ganglion cell dendrites were always postsynaptic to the labeled amacrine cells. It was more difficult to identify the presynaptic cell at synapses between labeled and unlabeled
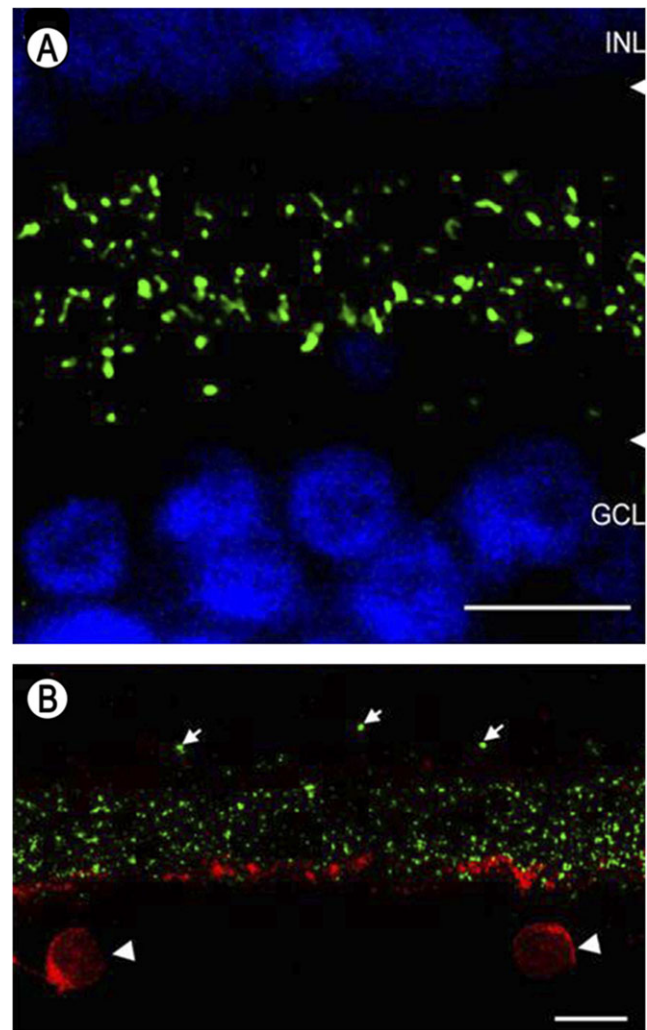
Fig. 1. Baboon retina labeled with rabbit antiserum against vGluT3. (**A**) A single optical section through the parafovea. Although the amacrine cell perikarya were unlabeled, there was robust labeling of the dendrites (green). The inner nuclear layer (INL) and ganglion cell layer (GCL) are labeled with DAPI (blue). (**B**) Stack of 7 optical sections. Most dendrites of vGluT3 cells (green) are located above the band of starburst amacrine cell dendrites in S4 labeled with antibody to choline acetyltransferase (ChAT, red), but there is some overlap between the two sets of dendrites. Note the vGluT3-positive primary dendrites (arrows) and the perikarya (arrowheads) of the starburst cells in the GCL. Scale bars = 10 μm.

amacrine cells. Clusters of vesicles were not a reliable indicator that vGluT3 cells were presynaptic because they were obscured by electron-dense peroxidase reaction product. Synapses like these were classified using the postsynaptic densities, instead. At synapses from labeled to unlabeled amacrine cells, the postsynaptic membrane density was thicker. When the labeled amacrine cell was postsynaptic, the synaptic density was thinner, and there were typically clusters of vesicles on the presynaptic side.

Synapses were assigned to the outer or inner sublamina based on their depth in the IPL. In all, 301 labeled synapses were observed (Table 1). The vast majority of synaptic input to the vGluT3 cells was from unlabeled amacrine cells. In the outer sublamina of the IPL, there were large synapses from electron-lucent amacrine cells onto primary dendrites of the vGluT3 cells (Fig. 3) and also synapses from other types of amacrine cells onto higher-order dendrites (Fig. 4A).
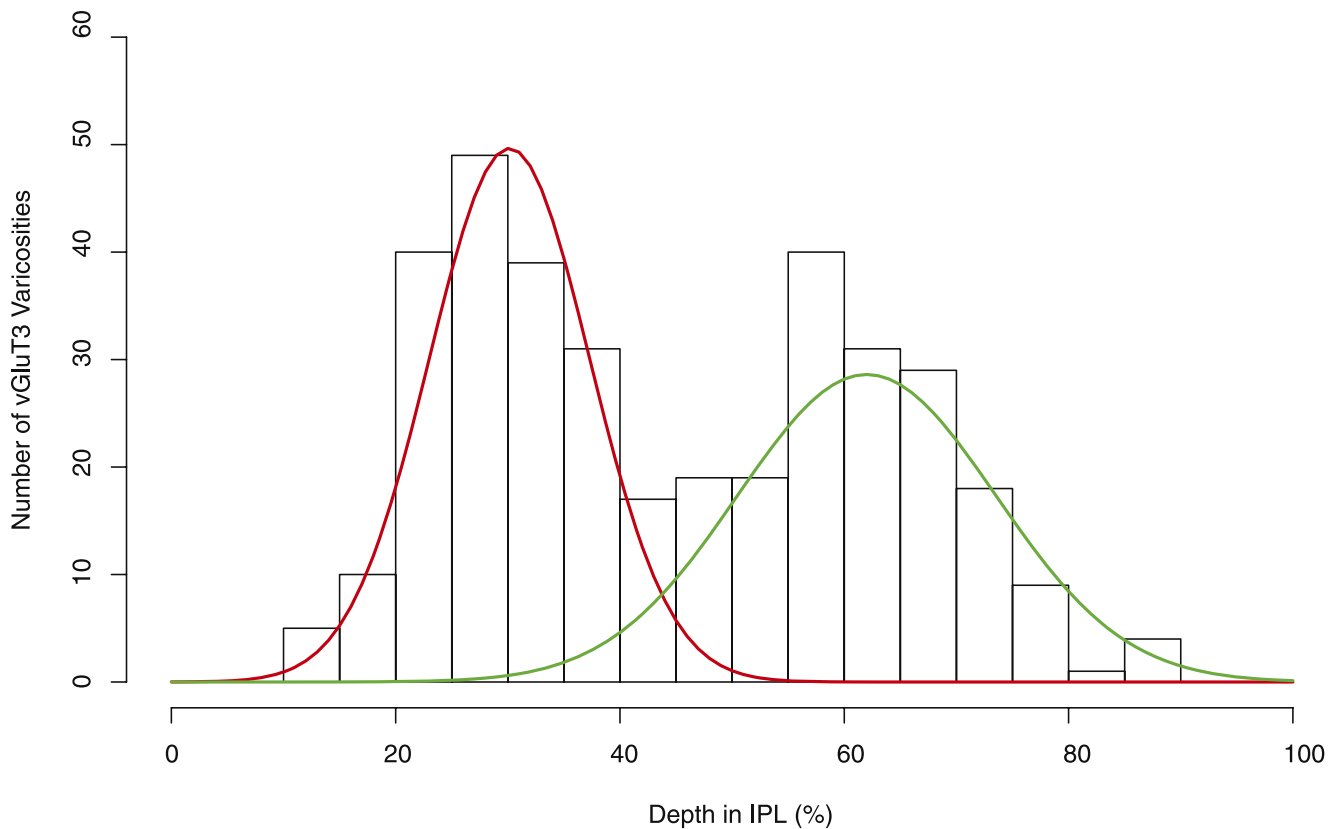
Fig. 2. The depths of labeled varicosities in the IPL are plotted with 0% being the lower border of the INL and 100% being the upper border of the GCL. The data were grouped into bins of 5% each and fitted with Gaussian functions with means ± standard deviations for the two distributions of 30 ± 7 (red, outer) and 62 ± 11 (green, inner). To demonstrate that the distribution was bimodal, a likelihood ratio test ($P < 0.0001$) was used.

There were an approximately equal number of inputs from amacrine cells to vGluT3 cells in the inner sublamina of the IPL. There were only two inputs to the labeled cells from bipolar cell axons at ribbon synapses; both were located in the inner sublamina of the IPL (Fig. 5A).

Approximately half of the output of the amacrine cells containing vGluT3 was directed to unlabeled amacrine cells (Fig. 4B). The numbers were similar in the outer and the inner sublamina.

Table 1. *The types of synapses found in the inner and outer halves of the IPL are compared. Two percentages are calculated for each type of synapse, the percentage of all synapses made or received by vGluT3 cells and the percentage of the total input to vGluT3 cells or total output from vGluT3 cells. All the synapses from bipolar cells to vGluT3 cells were in the inner half of the IPL, and all the synapses made by vGluT3 cells onto bipolar cells were in the outer half. Other types of synapses had very similar distributions in both halves*

		Outer			Inner	
INPUTS	*n*	% Total	% Inputs	*n*	% Total	% Inputs
Amacrine	77	26	46	89	30	53
Bipolar	0	0	0	2	<1	1
OUTPUTS	*n*	% Total	% Outputs	n	% Total	% Outputs
Amacrine	30	10	23	35	12	26
Bipolar	5	2	4	0	0	0
Ganglion	35	12	26	28	9	21

Only 4% of the synapses made by labeled amacrine cells were directed to bipolar cell axons. These synapses were not associated with synaptic ribbons, and all were located in the outer sublamina (Fig. 5B). The remainder of the output of the amacrine cells containing vGluT3 was directed to retinal ganglion cell dendrites (Fig. 6). There were approximately equal numbers of these synapses in the outer and the inner sublamina. Fig. 7 shows that, in some instances, the synaptic density in the postsynaptic cell was relatively thin, a slight thickening and an increase in the electron density of the plasma membrane, as in symmetric synapses found elsewhere in the central nervous system. In other cells receiving synapses from vGluT3 cells, the postsynaptic density extended 30 nm or more into the cytoplasm, as in asymmetric synapses (Peters et al., 1991; Harris & Weinberg, 2012).

Although there were only seven synapses between labeled amacrine cell dendrites and bipolar cell axons, the bipolar cells were consistently presynaptic in the inner sublamina and postsynaptic in the outer sublamina. The difference between the synapses between bipolar cells and vGluT3 cells in the outer sublamina and the inner sublamina was statistically significant ($P < 0.05$, Fisher exact test). There were no statistically significant differences between the two sublaminae in the relative numbers of synaptic connections of vGluT3 cells with other amacrine cells or with ganglion cells.

One type of bipolar cell that interacted with vGluT3 amacrine cells was the DB3a diffuse bipolar cell, which was labeled with antibodies to calbindin (Jacoby & Marshak, 2000; Puthussery et al., 2013). The amacrine cell dendrites labeled with antiserum to vGluT3
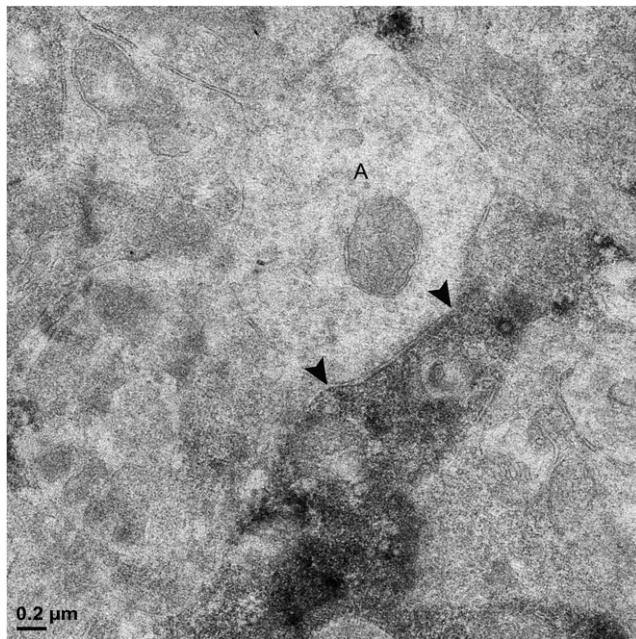
Fig. 3. A labeled primary dendrite of a vGluT3 amacrine cell receives a synapse from a large, electron-lucent amacrine cell (A) in the outer sublamina of the IPL. There are black arrowheads on either side of the synaptic density within the unlabeled profile.

made contacts with the labeled DB3a axon terminals (Fig. 8A). Based on the results with electron microscopy, it is likely that the bipolar cell axon terminals were postsynaptic.

Two types of amacrine cells that interact with vGluT3 amacrine cells were identified. In the inner sublamina, vGluT3 amacrine cell dendrites made contacts with the dendrites of starburst amacrine cells labeled with antibodies to choline acetyltransferase (Fig. 8B). Because starburst amacrine cells are both pre- and postsynaptic to unlabeled amacrine cells in macaque retina (Yamada et al., 2003), it was not possible to predict whether the vGluT3 cells were presynaptic, postsynaptic, or both. Dendrites containing vGluT3 also made contacts with the dendrites of AII amacrine cells labeled with antibodies to calretinin in both the outer and the inner sublamina (Fig. 8C). AII amacrine cells in macaque retina receive synapses from other types of amacrine cells, but they do not make chemical synapses onto amacrine cells (Wassle et al., 1995). Therefore, the vGluT3 amacrine cells are expected to be presynaptic to the AII cells at these contacts. The amacrine cells containing vGluT3 did not make contacts with the amacrine cells tracer-coupled to ON parasol ganglion cells (not illustrated).

The injected ganglion cells were classified as midget cells or parasol cells based on their characteristic morphology (Fig. 9). At a given eccentricity, the diameters of the perikarya and dendritic trees of parasol cells were larger than those of midget cells. In addition, the dendrites of parasol cells were more narrowly stratified and located closer to the center of the IPL than those of midget cells. Ganglion cells with dendrites ramifying in the outer half of the IPL were classified as OFF cells, and those with dendrites in the inner half of the IPL were classified as ON cells (Field & Chichilnisky, 2007). The sample included 11 ON parasol cells, 3 OFF parasol cells, 3 ON midget cells, and 2 OFF midget cells. The vGluT3 cells made contacts with parasol (Figs. 10 and 11) and midget (Figs. 12 and 13) ganglion cells. Both ON and OFF
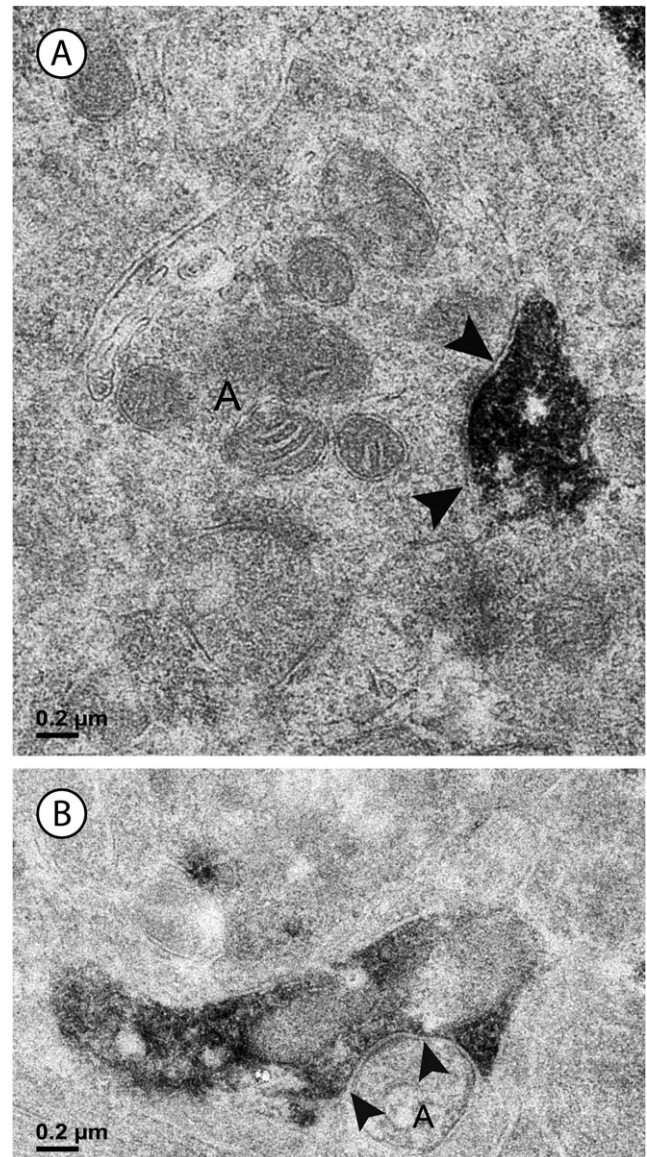
Fig. 4. Two labeled amacrine cell dendrites; there are black arrowheads on either side of the synaptic density within the unlabeled profiles. (**A**) An unlabeled amacrine cell (A) makes a synapse (arrowheads) onto a vGluT3 dendrite. Note the accumulation of vesicles and the concavity on presynaptic side of the synapse. (**B**) A labeled amacrine cell dendrite is presynaptic to another amacrine cell (A). The density on the postsynaptic side of the synapse is labeled with arrowheads.

subtypes of the two types of ganglion cells were contacted, and puncta containing the inhibitory synapse marker gephyrin were found at these sites.

The vGluT3 cells did not express glycine transporter 1 (GlyT1), although this marker of glycinergic transmission was readily detected in other amacrine cells (Fig. 14A). There were many sites where GlyT1-positive neurons made punctate contacts with vGluT3 cells. A similar pattern was observed in double label experiments with antibodies to GABA (Fig. 14B). There were many amacrine cells labeled, but these did not include the vGluT3 cells. There were many contacts between the two types of cells, a finding consistent with the results from electron microscopy.
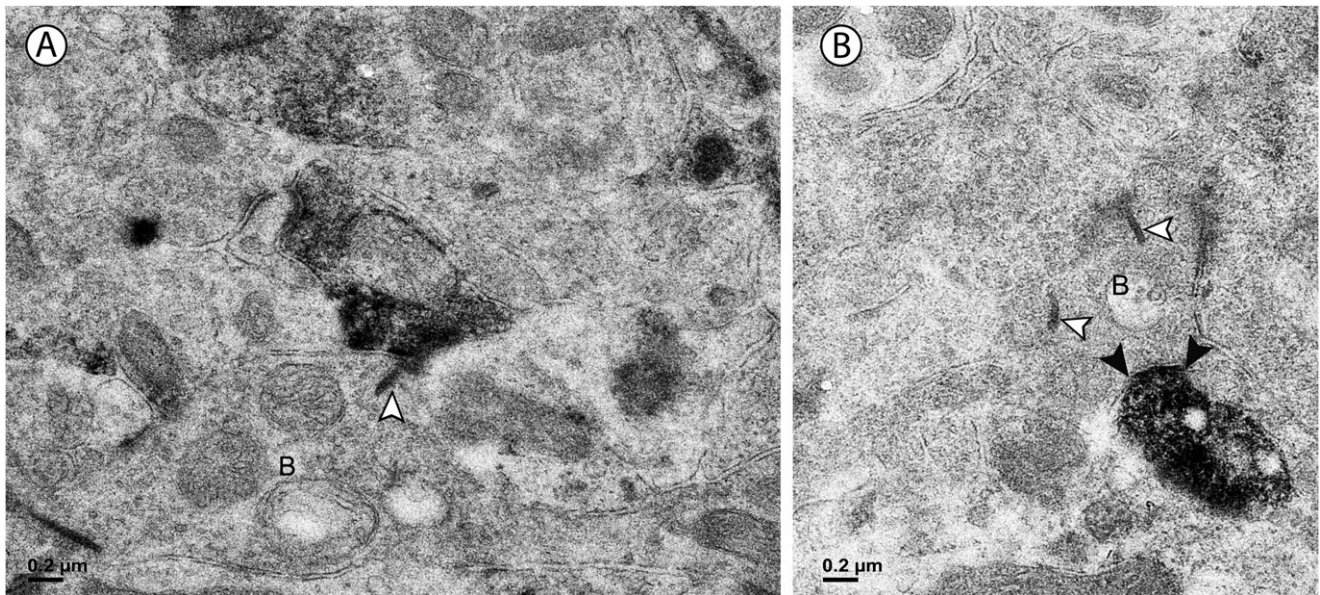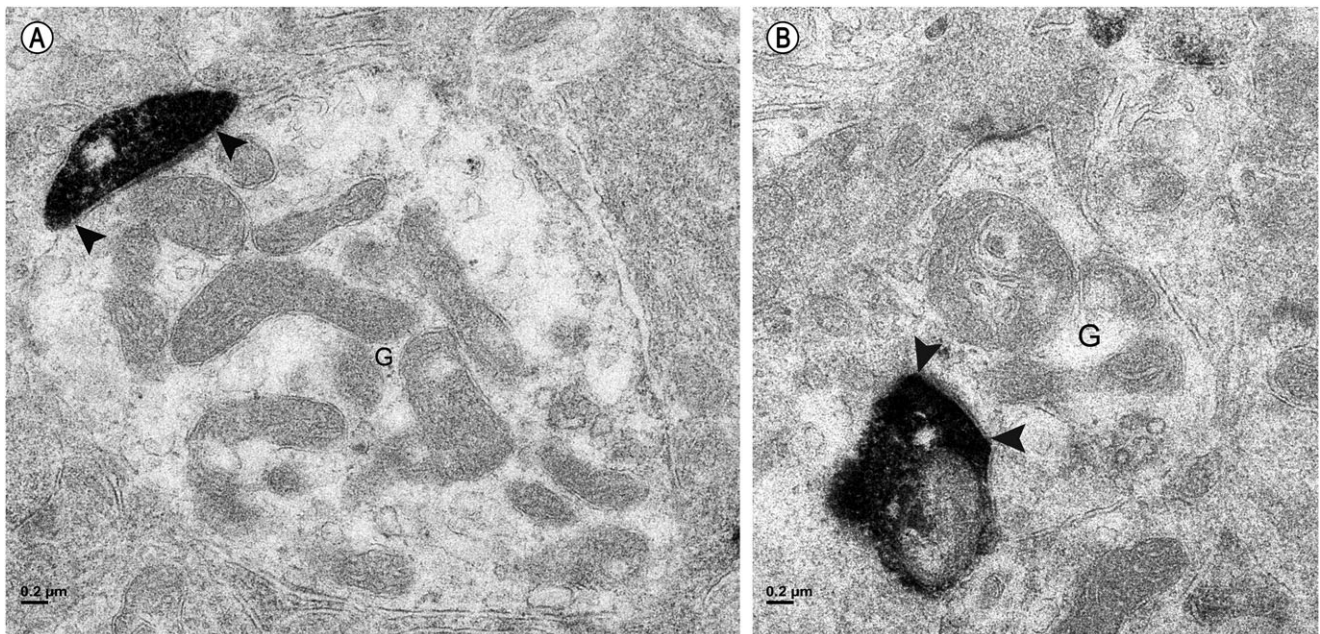
Fig. 5. (**A**) In the inner sublamina of the IPL, a vGluT3 cell dendrite receives a synapse from a bipolar cell axon (B) associated with a ribbon (white arrowhead). (**B**) In the outer sublamina of the IPL, a bipolar cell axon (B) receives a synapse from a labeled amacrine cell (black arrowheads). Note the synaptic ribbons (white arrowheads); these were not associated with labeled dendrites in this sublamina.

Discussion

Morphology of vGluT3 cells

The vGluT3 amacrine cells had varicose dendrites that ramified in two, relatively broad strata (S) that corresponded roughly with S2 and S4; there were very few labeled dendrites in the center of the IPL. The vGluT3 cells closely resembled knotty bistratified type 1 cells identified in macaque retina using the Golgi method (Mariani, 1990). The vGluT3 cells could readily be distinguished from several other types of narrow-field amacrine cells described previously in

primate retinas. They were morphologically different from AII amacrine cells, which have larger primary dendrites, lobular dendrites in S1 and S2 and arboreal dendrites in S5 (Mariani, 1990; Kolb et al., 1992), and they did not contain immunoreactive calretinin (Wassle et al., 1995; Mills & Massey, 1999). They were clearly different from A8 amacrine cells, which have arboreal dendrites ramifying in S1 and lobular dendrites extending to S3 and S4 (Kolb et al., 1992; Neumann & Haverkamp, 2013). They were also different from the knotty type 2 amacrine cells, also known as A3 cells. The knotty type 2 cells ramified mainly in S2 and had distinctive, indented varicosities that were larger than those of the vGluT3 cells

Fig. 6. (**A**) In the outer sublamina of the IPL, a labeled amacrine cell dendrite makes a synapse (arrowheads) onto a large ganglion cell dendrite (G). (**B**) In the inner sublamina of the IPL, a ganglion cell dendrite (G) receives a synapse (arrowheads) from a labeled amacrine cell.
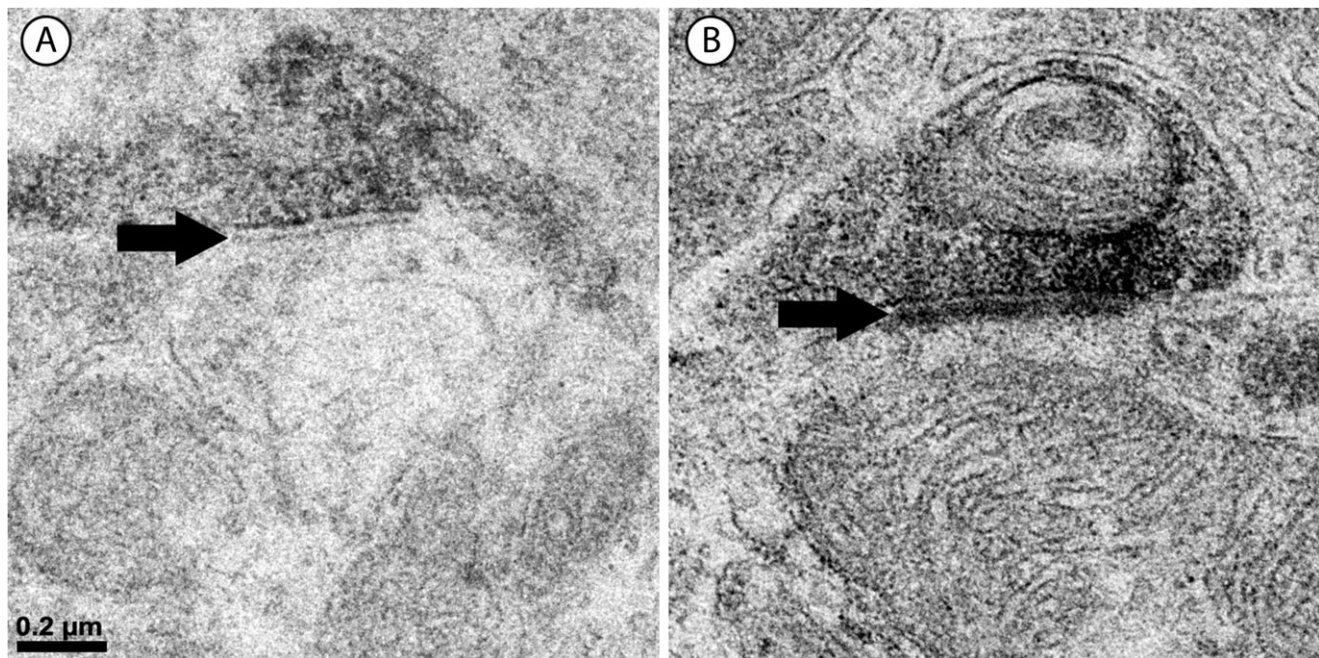
Fig. 7. Labeled amacrine dendrites make two different types of synapses. (**A**) The postsynaptic density (black arrow) here is relatively thin, only an increase in electron density of the plasma membrane. This is typical of symmetric synapses in the central nervous system. (**B**) The postsynaptic density (black arrow) here extends approximately 40 nm into the cytoplasm, as in asymmetric synapses elsewhere in the central nervous system.

(Klump et al., 2009). However, the vGluT3 cells might resemble A4 cells described previously in human retinas using the Golgi method. Although the A4 cells were described originally as broadly stratified rather than bistratified, they are similar to vGluT3 cells in other respects (Kolb et al., 1992).

vGluT3 amacrine cells in other mammals

Amacrine cells containing vGluT3 have been described previously in rats, mice, and cats, and in most respects, their morphology was very similar to those in primates. The major difference was in the inputs they received from bipolar cells. In one electron microscopic immunolabeling study of rat retina, inputs from cone bipolar cells were seen in both the inner and outer halves of the IPL (Haverkamp & Wassle, 2004). Two other studies using this technique also reported bipolar inputs but did not specify the level in the IPL where they occurred in either the rat retina (Johnson et al., 2004) or the cat retina (Fyk-Kolodziej et al., 2004). In an electrophysiological study of vGluT3 cells in mouse retina, glutamatergic excitatory inputs from bipolar cells were detected only at the offset of light stimuli, a finding suggesting that these originated in the outer half of the IPL (Grimes et al., 2011). In our study of the baboon retina, on the other hand, inputs from bipolar cells were only detected in the inner half of the IPL. A subset of retinal ganglion cells were labeled using a different antibody to vGluT3 in the human retina (Gong et al., 2006), but we did not see these in baboon retinas.

Synapses with ganglion cells

One major finding of the electron microscopic study was that vGluT3 cells in baboon retina directed more than half of their output to retinal ganglion cell dendrites. Unlike primate bipolar cells, vGluT3 narrow-field amacrine cells did not appear to be selective in their contacts with ganglion cells. The postsynaptic ganglion cells included midget ganglion cells of both ON and OFF types. Both the subtypes of midget ganglion cells express glycine receptors containing $\alpha 1$ subunits (Grunert & Ghosh, 1999; Grunert, 2000; Lin et al., 2000), and one type of presynaptic glycinergic amacrine cell has already been described. Multistratified amacrine cells containing relatively low levels of both calretinin and parvalbumin are presynaptic to ON midget ganglion cells (Kolb et al., 2002). Amacrine cells containing vGluT3 were also presynaptic to ON and OFF parasol cells. Dendrites of both subtypes have puncta containing the $\alpha 1$ subunit of the glycine receptor (Grunert & Ghosh, 1999). Two glycinergic amacrine cell types already known to be presynaptic to OFF parasol cells are AII cells and knotty type 2 cells (Bordt et al., 2006; Klump et al., 2009).

Synapses with bipolar cells and amacrine cells

There were very few synaptic interactions between vGluT3 cells and bipolar cells; these comprised only 2% of the sample in our electron microscopic study. Nevertheless, the difference between the synapses in the inner and outer halves of the IPL was unambiguous and statistically significant. The bipolar cells were always presynaptic to vGluT3 cells in the inner half of the IPL and always postsynaptic in the outer half. One of the postsynaptic targets was identified as the DB3a diffuse bipolar cells, which are presynaptic to OFF parasol cells (Jacoby et al., 2000; Puthussery et al., 2013). Because the vGluT3 only receive inputs from bipolar cells in the inner half of the IPL, they are expected to depolarize in response to increments in light intensity. If their resting membrane potential is relatively depolarized, as it is in vGluT3 cells of mice, they might also release neurotransmitter spontaneously (Grimes et al., 2011).
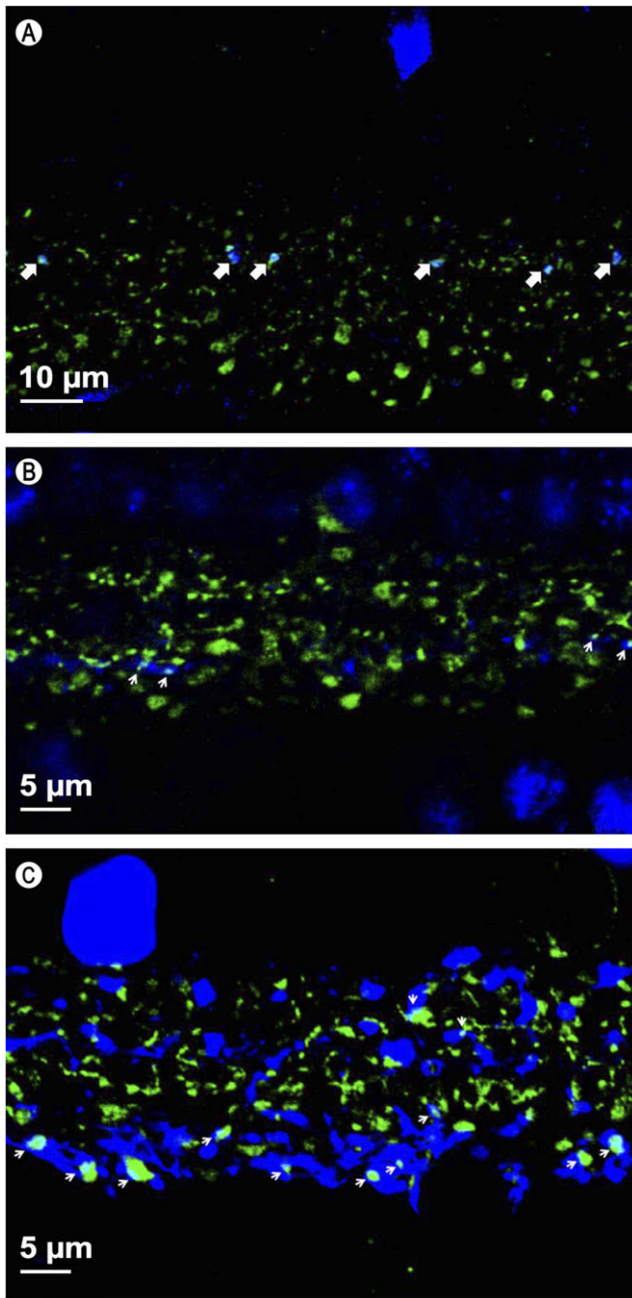
Fig. 8. (A) In the outer sublamina of the IPL, vGluT3-positive amacrine cell dendrites (green) make contacts with axon terminals of calbindin-positive DB3a bipolar cells (blue), and some of the contacts (aqua) are labeled with arrows. This is a single, 0.5 μm optical section, as are all the images that follow. (B) In the inner sublamina of the IPL, dendrites containing immunoreactive choline acetyltransferase (blue) make contacts (arrows) with dendrites of vGluT3 cells (green). (C) Dendrites containing immunoreactive calretinin (blue) make contacts (arrows) with dendrites of vGluT3 cells (green) in both halves of the IPL. Because AII cells do not make synapses onto other amacrine cells, the vGluT3 cells should be presynaptic there.

Over 99% of the synapses onto vGluT3 cells were from other amacrine cells, with approximately equal numbers of inputs in the inner and outer halves of the IPL. The large synapses from amacrine cells onto the primary dendrites suggest that the entire vGluT3 cell might be inhibited under some conditions. One candidate to provide
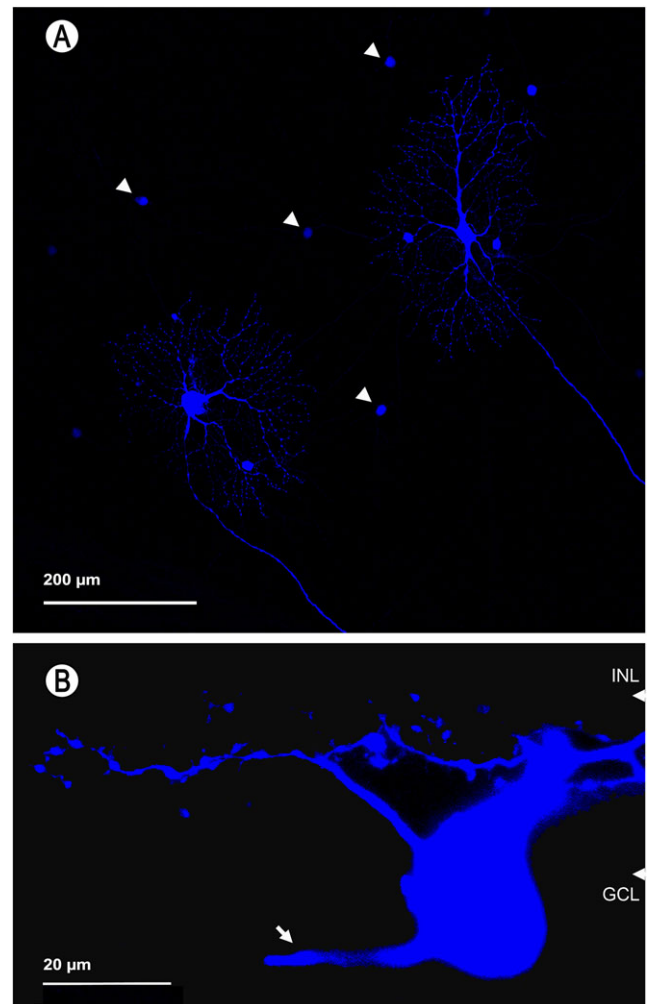
Fig. 9. Baboon retinal ganglion cells injected intracellularly with Neurobiotin. (A) Two ON parasol cells were injected and are illustrated in a flat mount preparation. In addition to the ganglion cells, perikarya of tracer-coupled amacrine cells (arrowheads) are visible. (B) An OFF midget ganglion cell was injected, and it is illustrated in a vertical, vibratome section. The axon is labeled with an arrow, and the boundaries of the IPL are marked with arrowheads. INL = inner nuclear layer and GCL = ganglion cell layer.

this input was identified in our light microscopic study; starburst cells may be among the presynaptic amacrine cells in S4. Starburst cells are both presynaptic and postsynaptic to amacrine cells in macaque retina (Yamada et al., 2003), and, therefore, it was not possible to predict whether the vGluT3 cells or the starburst cells were presynaptic. Based on the results from the mouse retina, type two tyrosine hydroxylase-positive cells might also be among the presynaptic amacrine cells (Knop et al., 2011).

Approximately half of the output of vGluT3 cells was directed to other amacrine cells, and one of these, the AII amacrine cell, was identified in our light microscopic study. The AII amacrine cells are expected to be postsynaptic at the contacts with vGluT3 cells based on results from two previous studies in primate retinas. AII cells receive synapses from amacrine cells but do not make chemical synapses onto other amacrine cells (Wassle et al., 1995). AII cells express α-2 glycine receptors at sites where they appear to be postsynaptic, and the same receptors are found in puncta where vGluT3 cells appear to be presynaptic (Jusuf et al., 2005).
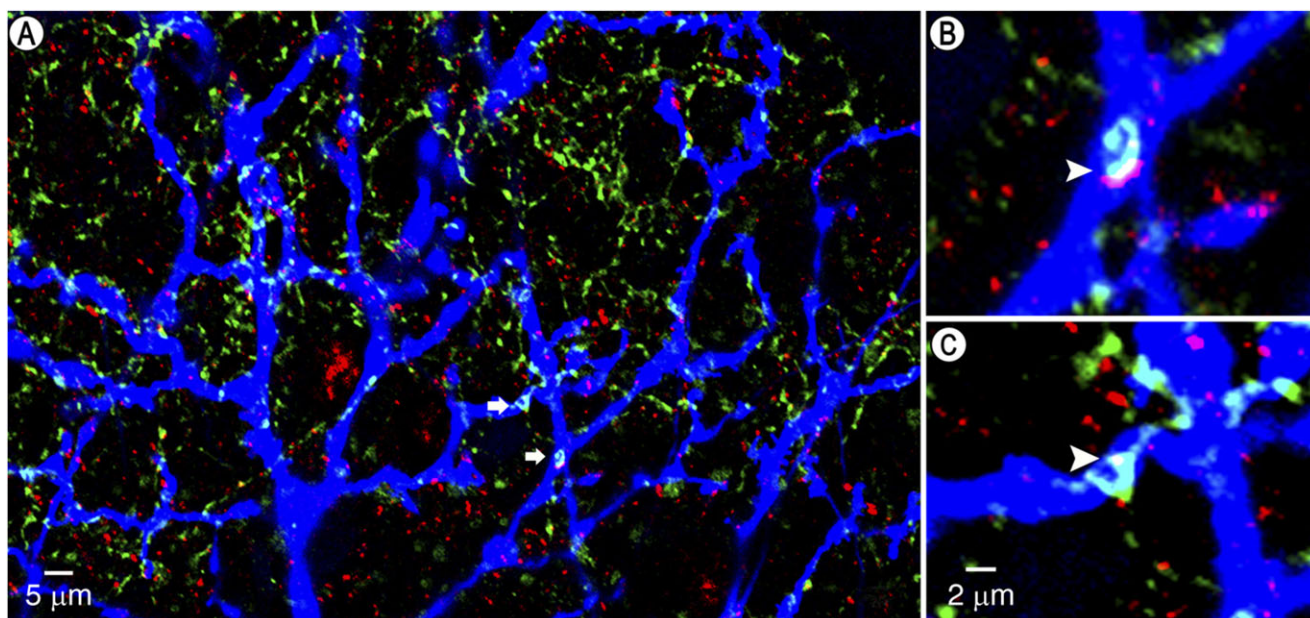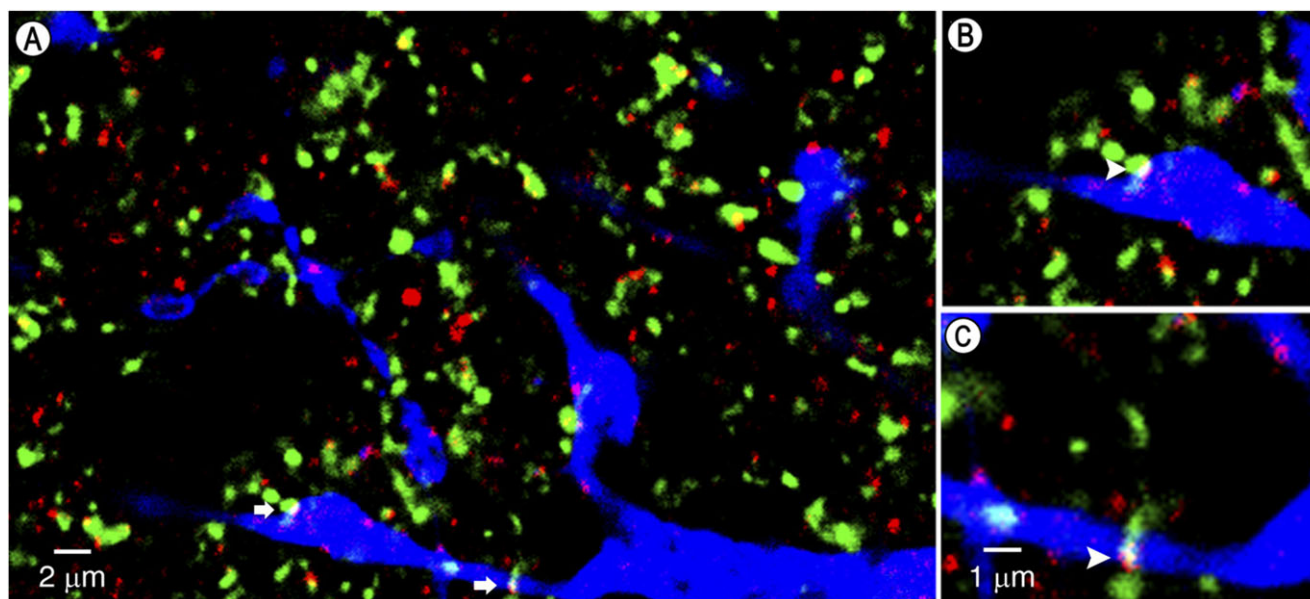
Fig. 10. Horizontal, optical section of the inner sublamina. (**A**) ON parasol ganglion cells (blue) are contacted (arrows) by vGluT3 cells (green), and puncta containing the inhibitory synapse marker gephyrin (red) are found there. (**B** and **C**) The contacts (arrowheads) are shown at higher magnification.

Neurotransmitters of vGluT3 cells

The vGluT3 cells were not labeled with antibody to GABA, as in previous studies of rodent retina (Haverkamp & Wassle, 2004; Johnson et al., 2004). The vGluT3 cells did not contain immunoreactive ChAT and were morphologically different from the cholinergic amacrine cells described previously (Rodieck & Marshak, 1992; Yamada et al., 2003). The vGluT3 cells did not resemble wide-field amacrine cells labeled with antibodies to tyrosine hydroxylase, either the dopaminergic type 1 cells or the GABAergic

type 2 cells (Mariani & Hokoc, 1988). Three lines of evidence suggest that vGluT3 cells in baboons use an excitatory amino acid neurotransmitter. The vGluT3 amacrine cells contain immunoreactive glutamate (Haverkamp & Wassle, 2004), as do many other types of amacrine cells in primates (Kalloniatis et al., 1996). In mice, dendrites of vGluT3 cells are closely associated with puncta containing metabotropic glutamate receptor 4 (Johnson et al., 2004), and they make excitatory glutamatergic synapses onto several types of retinal ganglion cells (Lee et al., 2014). An alternative explanation is that glutamate transported by vGluT3 enhances

Fig. 11. Horizontal, optical section of the outer sublamina. (**A**) An OFF parasol ganglion cell (blue) is contacted (arrows) by vGluT3 cells (green), and puncta containing the inhibitory synapse marker gephyrin (red) are found there. (**B** and **C**) The contacts (arrowheads) are shown at higher magnification.
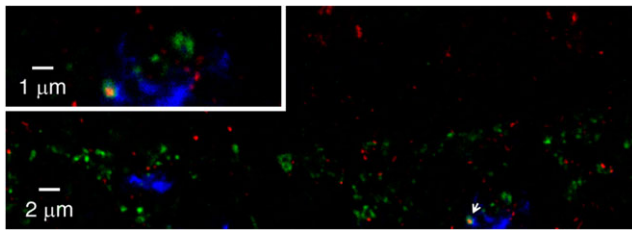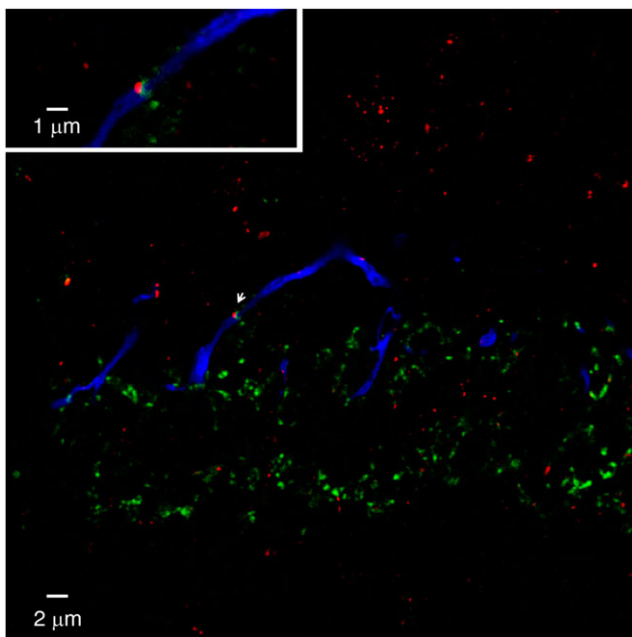
Fig. 12. An ON midget ganglion cell (blue) is contacted (arrow) by a vGluT3 cell (green), and a punctum containing the inhibitory synapse marker gephyrin (red) is found there. Inset: The contact is shown at higher magnification.

transport of the primary neurotransmitter into synaptic vesicles (El Mestikawy et al., 2011).

The vGluT3 amacrine cells in rodent retinas contain immunoreactive glycine (Haverkamp & Wassle, 2004; Johnson et al., 2004). However, even though other amacrine cells in baboon retina were well-labeled with antibodies to GlyT1, the amacrine cells containing vGluT3 were not. The same was true in the rat retina; there was weak labeling of the vGluT3 cell perikarya with antibody to GlyT1 and none on their dendrites (Haverkamp & Wassle, 2004). It is possible that vGluT3 cells use a different plasma membrane glycine transporter or that the GlyT1 of vGluT3 cells is not immunoreactive. A third possibility is that the vGluT3 cells do not have a plasma membrane glycine transporter; i.e., they synthesize and release glycine but do not take it up (Deniz et al., 2011).

In this study, we showed that puncta containing gephyrin, an inhibitory synapse marker (Fritschy et al., 2008; Tyagarajan & Fritschy, 2014), were located at contacts between vGluT3 cells and retinal ganglion cells. Because midget and parasol ganglion cells are never presynaptic in the IPL, the gephyrin-IR puncta must be on the postsynaptic side at these contacts (Dowling & Boycott, 1966; Kolb & Dekorver, 1991; Calkins et al., 1994; Jacoby et al., 1996;

Fig. 13. An OFF midget ganglion cell (blue) is contacted (arrow) by a vGluT3 cell (green), and a punctum containing the inhibitory synapse marker gephyrin (red) is found there. The contact (arrowhead) is shown at higher magnification in the inset.
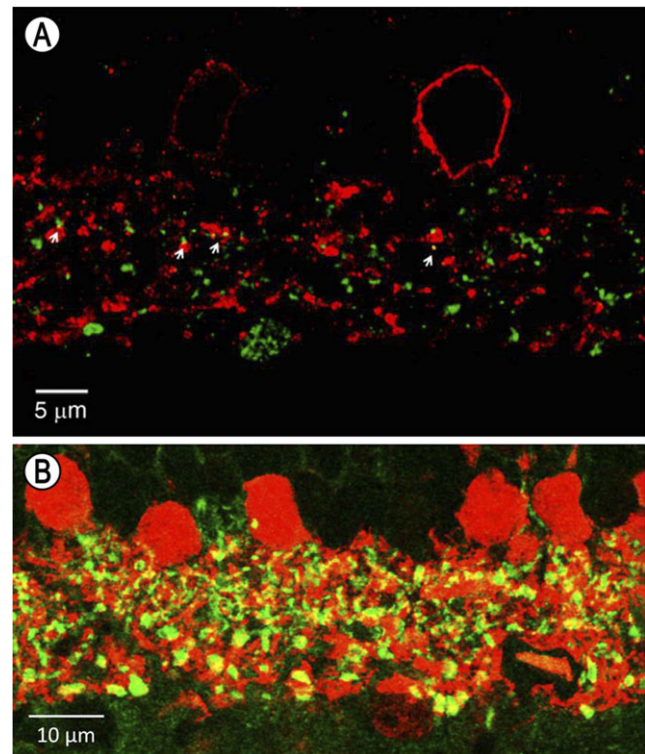
Fig. 14. (**A**) Amacrine cells were labeled with antibody to vesicular glutamate transporter 1 (red), but these did not include the vGluT3 cells (green). There were punctate contacts between the two types of cells (arrows). (**B**) Amacrine cells were labeled with antibody to GABA (red), but these did not include the vGluT3 cells (green). There were numerous punctate contacts between the two types of cells (yellow).

Marshak et al., 2002; Kolb & Marshak, 2003; Bordt et al., 2006; Calkins & Sterling, 2007). There is also evidence from the literature suggesting that vGluT3 cells use glycine as their neurotransmitter or, possibly, as a cotransmitter. In the cat retina, the vGluT3 cells make synapses with the symmetric densities characteristic of inhibitory synapses (Fyk-Kolodziej et al., 2004). Puncta containing the α2 subunit of the glycine receptor are found inside the presumed postsynaptic cells at appositions with the dendrites of the vGluT3 cells in primates (Jusuf et al., 2005) and in mice (Knop et al., 2011). We observed the same pattern of labeling in this study using antibody to gephyrin.

At synapses made by the vGluT3 cells in this study, some of the postsynaptic densities were relatively thin, as in symmetric synapses. At the other synapses made by the vGluT3 cells, the postsynaptic densities were relatively thick, as in asymmetric synapses, and these may correspond to the rare, conventional synapses with E-face particles in the postsynaptic membrane that were observed in the macaque IPL in a study using freeze-fracture (Raviola & Raviola, 1982). In the brain, symmetric synapses are known to be inhibitory and asymmetric synapses are known to be excitatory (Peters et al., 1991; Harris & Weinberg, 2012). One possible explanation that would account for all the results from this study and those reported previously is that the vGluT3 cells release glycine at some of their synapses and glutamate at others. Recently, a similar phenomenon was discovered in the lateral habenula of the rat brain. Single axons projecting there from the ventral tegmental area make both symmetrical synapses associated with markers of GABAergic transmission and asymmetric synapses associated

with markers of glutamatergic transmission (Root et al., 2014). Co-release of GABA and glutamate has also been reported in granule cells of the rat olfactory bulb (Didier et al., 2001). Similar correlated anatomical and physiological studies on the retina will be required to test this hypothesis.

Acknowledgments

References

Bordt, A.S., Hoshi, H., Yamada, E.S., Perryman-Stout, W.C. & Marshak, D.W. (2006). Synaptic input to OFF parasol ganglion cells in macaque retina. *The Journal of Comparative Neurology* **498**, 46–57.

Calkins, D.J., Schein, S.J., Tsukamoto, Y. & Sterling, P. (1994). M and L cones in macaque fovea connect to midget ganglion cells by different numbers of excitatory synapses. *Nature* **371**, 70–72.

Calkins, D.J. & Sterling, P. (2007). Microcircuitry for two types of achromatic ganglion cell in primate fovea. *The Journal of Neuroscience* **27**, 2646–2653.

Deniz, S., Wersinger, E., Schwab, Y., Mura, C., Erdelyi, F., Szabo, G., Rendon, A., Sahel, J.A., Picaud, S. & Roux, M.J. (2011). Mammalian retinal horizontal cells are unconventional GABAergic neurons. *Journal of Neurochemistry* **116**, 350–362.

Didier, A., Carleton, A., Bjaalie, J.G., Vincent, J.D., Ottersen, O.P., Storm-Mathisen, J. & Lledo, P.M. (2001). A dendrodendritic reciprocal synapse provides a recurrent excitatory connection in the olfactory bulb. *Proceedings of the National Academy of Sciences of the United States of America* **98**, 6441–6446.

Dowling, J.E. & Boycott, B.B. (1966). Organization of the primate retina: Electron microscopy. *Proceedings of the Royal Society of London. Series B, Biological Sciences* **166**, 80–111.

El Mestikawy, S., Wallen-Mackenzie, A., Fortin, G.M., Descarries, L. & Trudeau, L.E. (2011). From glutamate co-release to vesicular synergy: Vesicular glutamate transporters. *Nature Reviews. Neuroscience* **12**, 204–216.

Field, G.D. & Chichilnisky, E.J. (2007). Information processing in the primate retina: Circuitry and coding. *Annual Review of Neuroscience* **30**, 1–30.

Fritschy, J.M., Harvey, R.J. & Schwarz, G. (2008). Gephyrin: Where do we stand, where do we go? *Trends in Neurosciences* **31**, 257–264.

Fyk-Kolodziej, B., Dzhagaryan, A., Qin, P. & Pourcho, R.G. (2004). Immunocytochemical localization of three vesicular glutamate transporters in the cat retina. *The Journal of Comparative Neurology* **475**, 518–530.

Gastinger, M.J., Barber, A.J., Vardi, N. & Marshak, D.W. (2006). Histamine receptors in mammalian retinas. *Journal of Comparative Neurology* **495**, 658–667.

Gong, J., Jellali, A., Mutterer, J., Sahel, J.A., Rendon, A. & Picaud, S. (2006). Distribution of vesicular glutamate transporters in rat and human retina. *Brain Research* **1082**, 73–85.

Grimes, W.N., Seal, R.P., Oesch, N., Edwards, R.H. & Diamond, J.S. (2011). Genetic targeting and physiological features of VGLUT3+ amacrine cells. *Visual Neuroscience* **28**, 381–392.

Grunert, U. (1997). Anatomical evidence for rod input to the parvocellular pathway in the visual system of the primate. *The European Journal of Neuroscience* **9**, 617–621.

Grunert, U. (2000). Distribution of GABA and glycine receptors on bipolar and ganglion cells in the mammalian retina. *Microscopy Research and Technique* **50**, 130–140.

Grunert, U. & Ghosh, K.K. (1999). Midget and parasol ganglion cells of the primate retina express the alpha1 subunit of the glycine receptor. *Visual Neuroscience* **16**, 957–966.

Harris, K.M. & Weinberg, R.J. (2012). Ultrastructure of synapses in the mammalian brain. *Cold Spring Harbor Perspectives in Biology* **4**, 1–30.

Haverkamp, S. & Wassle, H. (2004). Characterization of an amacrine cell type of the mammalian retina immunoreactive for vesicular glutamate transporter 3. *The Journal of Comparative Neurology* **468**, 251–263.

Jacoby, R., Stafford, D., Kouyama, N. & Marshak, D. (1996). Synaptic inputs to ON parasol ganglion cells in the primate retina. *The Journal of Neuroscience* **16**, 8041–8056.

Jacoby, R.A. & Marshak, D.W. (2000). Synaptic connections of DB3 diffuse bipolar cell axons in macaque retina. *The Journal of Comparative Neurology* **416**, 19–29.

Jacoby, R.A., Wiechmann, A.F., Amara, S.G., Leighton, B.H. & Marshak, D.W. (2000). Diffuse bipolar cells provide input to OFF parasol ganglion cells in the macaque retina. *The Journal of Comparative Neurology* **416**, 6–18.

Johnson, J., Sherry, D.M., Liu, X., Fremeau, R.T., Jr., Seal, R.P., Edwards, R.H. & Copenhagen, D.R. (2004). Vesicular glutamate transporter 3 expression identifies glutamatergic amacrine cells in the rodent retina. *The Journal of Comparative Neurology* **477**, 386–398.

Jusuf, P.R., Haverkamp, S. & Grunert, U. (2005). Localization of glycine receptor alpha subunits on bipolar and amacrine cells in primate retina. *The Journal of Comparative Neurology* **488**, 113–128.

Kalloniatis, M., Marc, R.E. & Murry, R.F. (1996). Amino acid signatures in the primate retina. *The Journal of Neuroscience* **16**, 6807–6829.

Klump, K.E., Zhang, A.J., Wu, S.M. & Marshak, D.W. (2009). Parvalbumin-immunoreactive amacrine cells of macaque retina. *Visual Neuroscience* **26**, 287–296.

Knop, G.C., Feigenspan, A., Weiler, R. & Dedek, K. (2011). Inputs underlying the ON-OFF light responses of type 2 wide-field amacrine cells in TH::GFP mice. *The Journal of Neuroscience* **31**, 4780–4791.

Kolb, H. & Dekorver, L. (1991). Midget ganglion cells of the parafovea of the human retina: A study by electron microscopy and serial section reconstructions. *The Journal of Comparative Neurology* **303**, 617–636.

Kolb, H., Linberg, K.A. & Fisher, S.K. (1992). Neurons of the human retina: A Golgi study. *The Journal of Comparative Neurology* **318**, 147–187.

Kolb, H. & Marshak, D. (2003). The midget pathways of the primate retina. *Documenta Ophthalmologica* **106**, 67–81.

Kolb, H., Zhang, L., Dekorver, L. & Cuenca, N. (2002). A new look at calretinin-immunoreactive amacrine cell types in the monkey retina. *The Journal of Comparative Neurology* **453**, 168–184.

Koontz, M.A. & Hendrickson, A.E. (1987). Stratified distribution of synapses in the inner plexiform layer of primate retina. *Journal of Comparative Neurology* **263**, 581–592.

Lee, S., Chen, L., Chen, M., Ye, M., Seal, R.P. & Zhou, Z.J. (2014). An unconventional glutamatergic circuit in the retina formed by vGluT3 amacrine cells. *Neuron* **84**, 708–715.

Lin, B., Martin, P.R., Solomon, S.G. & Grunert, U. (2000). Distribution of glycine receptor subunits on primate retinal ganglion cells: A quantitative analysis. *The European Journal of Neuroscience* **12**, 4155–4170.

Mariani, A.P. (1990). Amacrine cells of the rhesus monkey retina. *The Journal of Comparative Neurology* **301**, 382–400.

Mariani, A.P. & Hokoc, J.N. (1988). Two types of tyrosine hydroxylase-immunoreactive amacrine cell in the rhesus monkey retina. *The Journal of Comparative Neurology* **276**, 81–91.

Marshak, D.W., Yamada, E.S., Bordt, A.S. & Perryman, W.C. (2002). Synaptic input to an on parasol ganglion cell in the macaque retina: A serial section analysis. *Visual Neuroscience* **19**, 299–305.

Mills, S.L. & Massey, S.C. (1999). AII amacrine cells limit scotopic acuity in central macaque retina: A confocal analysis of calretinin labeling. *The Journal of Comparative Neurology* **411**, 19–34.

Mills, S.L., Xia, X.B., Hoshi, H., Firth, S.I., Rice, M.E., Frishman, L.J. & Marshak, D.W. (2007). Dopaminergic modulation of tracer coupling in a ganglion-amacrine cell network. *Visual Neuroscience* **24**, 593–608.

Neumann, S. & Haverkamp, S. (2013). Characterization of small-field bistratified amacrine cells in macaque retina labeled by antibodies against synaptotagmin-2. *The Journal of Comparative Neurology* **521**, 709–724.

Peters, A., Palay, S.L. & Webster, H.d. (1991). *The Fine Structure of the Nervous System: Neurons and Their Supporting Cells*. New York: Oxford University Press.

Puthussery, T., Venkataramani, S., Gayet-Primo, J., Smith, R.G. & Taylor, W.R. (2013). NaV1.1 channels in axon initial segments of bipolar cells augment input to magnocellular visual pathways in the primate retina. *The Journal of Neuroscience* **33**, 16045–16059.

RAVIOLA, E. & RAVIOLA, G. (1982). Structure of the synaptic membranes in the inner plexiform layer of the retina: A freeze-fracture study in monkeys and rabbits. *The Journal of Comparative Neurology* **209**, 233–248.

REYNOLDS, E.S. (1963). The use of lead citrate at high pH as an electron-opaque stain in electron microscopy. *The Journal of Cell Biology* **17**, 208–212.

RODIECK, R.W. & MARSHAK, D.W. (1992). Spatial density and distribution of choline acetyltransferase immunoreactive cells in human, macaque, and baboon retinas. *The Journal of Comparative Neurology* **321**, 46–64.

ROOT, D.H., MEJIAS-APONTE, C.A., ZHANG, S., WANG, H.L., HOFFMAN, A.F., LUPICA, C.R. & MORALES, M. (2014). Single rodent mesohabenular axons release glutamate and GABA. *Nature Neuroscience* **17**, 1543–1551.

TYAGARAJAN, S.K. & FRITSCHY, J.M. (2014). Gephyrin: A master regulator of neuronal function? *Nature Reviews. Neuroscience* **15**, 141–156.

WASSLE, H., GRUNERT, U., CHUN, M.H. & BOYCOTT, B.B. (1995). The rod pathway of the macaque monkey retina: Identification of AII-amacrine cells with antibodies against calretinin. *The Journal of Comparative Neurology* **361**, 537–551.

WASSLE, H., HEINZE, L., IVANOVA, E., MAJUMDAR, S., WEISS, J., HARVEY, R.J. & HAVERKAMP, S. (2009). Glycinergic transmission in the Mammalian retina. *Frontiers in Molecular Neuroscience* **2**, 6.

YAMADA, E.S., DMITRIEVA, N., KEYSER, K.T., LINDSTROM, J.M., HERSH, L.B. & MARSHAK, D.W. (2003). Synaptic connections of starburst amacrine cells and localization of acetylcholine receptors in primate retinas. *The Journal of Comparative Neurology* **461**, 76–90.